The 7th International Supercritical CO_2 Power Cycles Symposium
February 21 – 24, 2022, San Antonio, Texas
Paper #185

A Methodology to Identify the Most Promising Concentrating Solar Power Layouts to be Integrated with Supercritical CO_2 Power Cycles

Salvatore Guccione
PhD Candidate
KTH Royal Institute of Technology
Stockholm, Sweden

Silvia Trevisan
PhD Candidate
KTH Royal Institute of Technology
Stockholm, Sweden

Rafael Guedez
Senior Researcher
KTH Royal Institute of Technology
Stockholm, Sweden

ABSTRACT

The integration of compact and high-efficient supercritical CO_2 (sCO_2) power blocks has been identified as one of the key alternatives for enhancing the economic viability, and the flexibility of Concentrating Solar Power (CSP) plants. The present work aims at identifying and selecting the most promising CSP plant configurations that can be integrated with sCO_2 power blocks. Several sCO_2 – CSP layouts are identified, classified by the receiver heat transfer fluid and storage design, and benchmarked through a methodology developed by the authors. An analytical approach, based on purposely defined techno-economic criteria, is defined to benchmark each layout with an overall score. The following criteria are considered: maturity, low-cost potential, maximum temperature, safety, and system complexity. The overall score is then derived by combining the mentioned criteria and weighting factors. A comparative analysis is proposed, in which the higher the resulting overall score, the more attractive the layout was deemed. The CSP layout employing molten salts results in being the most attractive one, standing out for its maturity. The air- or particle-based configurations combined with packed beds or particle silos as storage are promising for their low-cost potential and high operating temperatures.

INTRODUCTION

The integration of compact and high-efficient sCO_2 power blocks can boost the CSP deployment by increasing the overall thermal efficiency and reducing costs [1]. A possible outline of the next generation of CSP systems is the state-of-the-art molten salt solar tower coupled with a sCO_2 power block as shown in Figure 1. Due to the industry experience, operating flexibility, and energy-storage efficiency, this configuration is a leading contender. However, owing to molten salt's decomposition around 580 °C, new development of advanced heat transfer fluids and storage technologies are necessary to evolve to higher temperatures to be able to reach thermal efficiencies superior to 50%. The present work introduces a novel methodology to identify and select the most promising CSP plant configurations that can be integrated with sCO_2 power blocks. Twenty-one sCO_2 – CSP layouts have been outlined and compared focusing on the receiver heat transfer fluid (HTF), and the storage technologies, while all layouts include a Brayton cycle with recompression and reheat. The considered HTFs are air, CO_2, molten salt, chloride salt, sodium, and particles. The storage designs included are molten salt tanks, chloride salt tanks, air/nitrogen/CO_2 packed- beds, encapsulated (or contained) Phase Change Materials (PCMs), thermochemical, and particle silos.

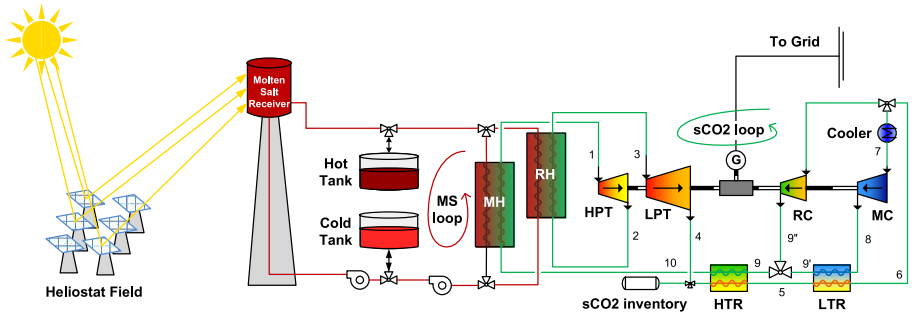

Figure 1: Schematic of the molten salt sCO_2-CSP layout

METHODOLOGY

To highlight the most promising layouts, an analytical approach, based on techno-economic criteria, has been built to benchmark each layout analyzed with an overall score (between 1 and 5). The higher the overall score, the more attractive will be the layout under investigation. Figure 2 shows the methodology developed to benchmark and support the selection of the 3 best configurations. Five scores are defined for each layout, namely the maturity score (S_{mat}), the potential low-cost score (S_{cost}), the safety score (S_{safe}), the complexity score (S_{comp}), and the maximum temperature score (S_{temp}). The overall score (S_o) can be calculated as the weighted average between all the aforementioned scores:

$$S_o = S_{mat} \cdot w_{mat} + S_{cost} \cdot w_{cost} + S_{safe} \cdot w_{safe} + S_{comp} \cdot w_{comp} + S_{temp} \cdot w_{temp} \quad (1)$$

where w_i indicates the weight for each score. The choice of the set of weights represents a key factor in the definition of the overall score and strongly influences the classification of the layouts. Therefore, for this purpose, three different weight combinations are considered and reported in Table 1. In this approach, maturity and cost are prioritized to guide the selection of the best CSP+sCO$_2$ system layouts. The combination Cost/Maturity represents the average between the combinations *Best for Maturity* and *Best for Cost*.

Table 1: Weight combinations for the overall score calculation

	Best for Maturity	**Cost/Maturity**	**Best for Cost**
Maturity Weight	0.5	0.4	0.3
Cost Weight	0.3	0.4	0.5
Temperature Weight	0.05	0.05	0.05
Safety Weight	0.1	0.1	0.1
Complexity Weight	0.05	0.050	0.050

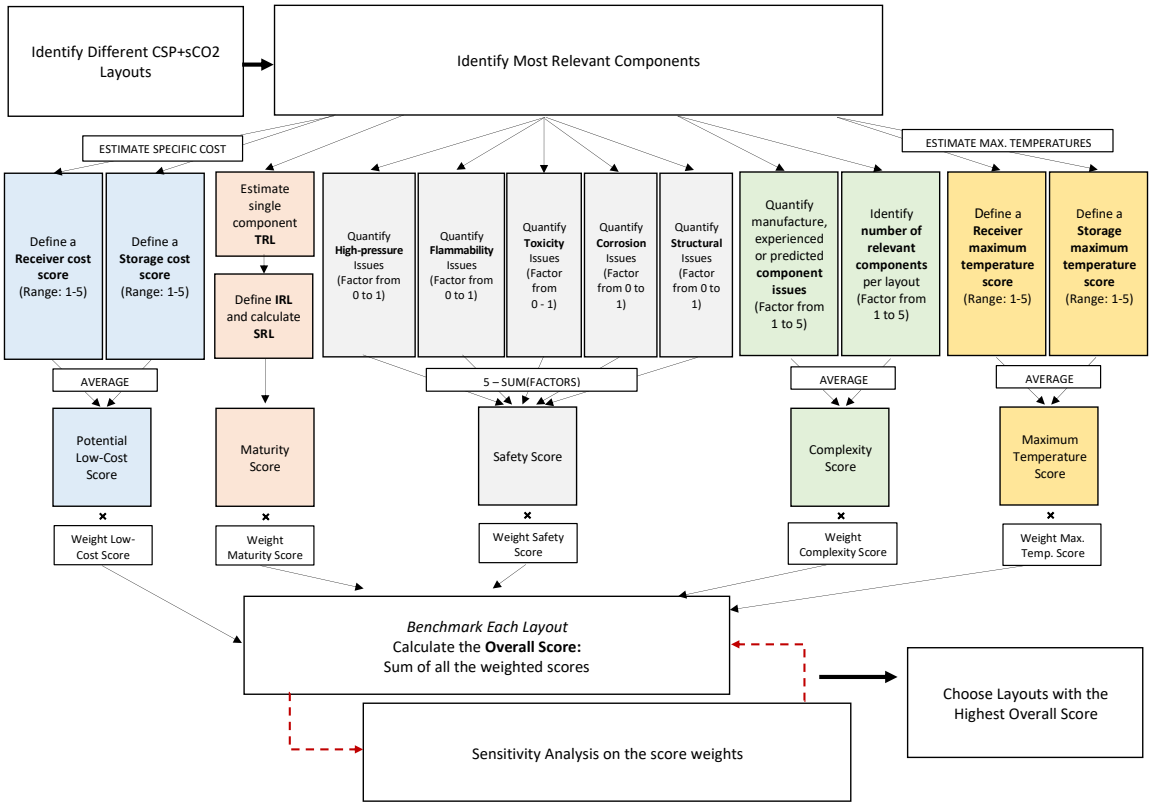

Figure 2: Schematic representation of layout selection methodology

The potential low-cost score (S_{cost}) is defined to compare the set of CSP+sCO2 layouts based on their expected capital expenditure. The highest score corresponds to the cheapest system. Assuming comparable solar field layouts and having adopted identical power block configurations only the receiver and tower and storage subsystems are considered for comparing the different layouts. The receiver cost score and the storage cost score have been defined based on the subsystem costs identified in the literature and reported in Table 2. The cost score for the receiver and the storage subsystems is calculated as shown in Equation (2) and (3) based on the lowest and the highest specific cost values (c_{min} and c_{max}). The potential low-cost score is calculated as the average between the aforementioned scores.

$$S_{cost,REC} = \frac{4 \cdot \left(c_{REC} - c_{REC,max}\right)}{c_{REC,min} - c_{REC,max}} + 1 \qquad (2) \qquad S_{cost,TES} = \frac{4 \cdot \left(c_{TES} - c_{TES,max}\right)}{c_{TES,min} - c_{TES,max}} + 1 \qquad (3)$$

The maturity of a system can be estimated by adopting the System Readiness Assessment (SRA) methodology [2]. The SRA approach defines the System Readiness Level (SRL), and it is based on the Technology Readiness Level (TRL) and the Integration Readiness Level (IRL) matrix. The TRL of the components has been estimated by the authors according to literature and coherently to the European Union (EU) TRL scale [3]. The assumed values are reported in Table 2, Table 3, and Table 4. The IRL is a metric to measure the integration maturity between two or more components. For a given system with *n* components, an IRL matrix ($n \times n$) is defined to consider the integration of the different components with each other. The IRL values ($IRL_{i,j}$) in the matrix range from 0 to 9, where zero is assigned for no integration between two specific components, while 9 is adopted for the integration of a component to itself ($IRL_{i,i}$).
The array of component SRL (SRL_c) is obtained by calculating the matrix product between the IRL and TRL and dividing each element by the number of integrations (m_i) of component *i* with every other component as shown in Equation (4). Each element of the array represents the readiness level of the component included in a specific system.

$$\begin{bmatrix} SRL_{c,1} \\ \vdots \\ SRL_{c,n} \end{bmatrix} = \begin{bmatrix} SRL_1/m_1 \\ \vdots \\ SRL_n/m_n \end{bmatrix} \quad where \quad \begin{bmatrix} SRL_1 \\ \vdots \\ SRL_n \end{bmatrix} = \begin{bmatrix} IRL_{1,1} & \cdots & IRL_{1,n} \\ \vdots & \ddots & \vdots \\ IRL_{n,1} & \cdots & IRL_{n,n} \end{bmatrix} \times \begin{bmatrix} TRL_1 \\ \vdots \\ TRL_n \end{bmatrix} \qquad (4)$$

Table 2: Assumptions for receiver and storage subsystems

	Type	TRL	Max T [°C]	Specific Cost [€/kW$_t$]	Toxicity	Flammability	High-pressure	Corrosion	Structural
Receiver/Tower	Molten Salt	9	600 [4]	128 [5]	0.10 [6]–[8]	0.00 [9]	0.00 [9]	0.25 [6]–[8]	0.00 [9]
	Air	6 [10]–[12]	1400 [9]	97 [1]	0.00	0.00	0.50	0.00	0.25
	Chloride Salt	3 [13]	800 [14]	205 [5]	0.25 [6]–[8]	0.00 [9]	0.00 [9]	1.00 [6]–[8]	0.00 [9]
	Sodium	6 [15]	850 [9]	199 [16]	0.25 [9]	1.00 [15]	0.00	0.25 [9]	0.00
	Particle	5 [17]	1000 [18]	105 [19]	0.00	0.00	0.00	0.00	0.25
	High-T CO_2	3 [20]	1200 [9]	130 [1], [5]	0.00	0.00	0.50	0.50 [9]	0.25
	sCO_2	2 [21], [22]	900 [9]	164 [5]	0.00	0.00	1.00	0.50 [9]	1.00 [23]
	Type	**TRL**	**Max T [°C]**	**Specific Cost [€/kWh$_t$]**	**Toxicity**	**Flammability**	**High-pressure**	**Corrosion**	**Structural**
Storage	Air Packed Bed	6 [24]	1000 [25]	8 [9]	0.00	0.00	0.80	0.00	0.30
	Moving Packed bed with particle bins	5 [5], [18]	1000 [9]	16 [19]	0.00	0.00	0.00	0.00	0.50 [18]
	Molten Salt Tanks	9 [24]	600 [9]	22 [5]	0.25 [26]	0.00	0.00	0.25 [26]	0.10 [26]
	Chloride Salt Tanks	4 [4]	800 [14]	52 [5]	0.25 [6]–[8]	0.00	0.00	1.00 [6]–[8]	0.25 [9]
	Nitrogen Packed Bed	6 [24]	1000 [25]	8 [9]	0.00	0.00	0.80	0.00	0.30
	CO_2 Packed Bed	5	1000 [25]	8 [9]	0.00	0.00	1.00	0.50 [9]	1.00
	Phase-Change Material (PCM - AlSi)	4 [24]	600 [5]	33 [5]	0.00	0.00	0.00	1.00	0.50
	Thermochemical	5 [24]	600	67 [27]	0.25	0.00	0.00	0.25	0.50
	Particle Silos	6 [17]	1000 [9]	8 [9]	0.00	0.00	0.00	0.00	0.40

Table 3: Assumptions for the heat exchangers

	Type	TRL	Complexity Factor
Heat Exchangers	Molten Salts - sCO_2	4	0.40
	Chloride Salts - sCO_2	3	0.80
	Sodium - Chloride Salts	3 [16]	0.90 [16]
	Sodium - Nitrogen	1	0.80
	Sodium - CO_2	1	0.80
	Particle - sCO_2	3 [28], [29]	0.60 [17]
	Air - sCO_2	4	0.40
	Sodium - sCO_2	3	1.00
	Particle – Air	4 [18]	0.50 [30], [31]
	CO_2 - sCO_2	4	0.40
	Nitrogen - sCO_2	4	0.40

Table 4: Assumptions for the other components

	Type	TRL	Complexity Factor
Other Components	Molten Salt EH	4 [32]	0.50
	Heliostats Field / PV	9	0.00
	Air/N Electric Heater	9 [9]	0.20 [9]
	CO_2 Electric Heater	8	0.30
	Burner for sCO_2	5	0.70
	Low/High Temp. Fan	9	0.00/0.25
	Molten Salts Pump	9	0.25
	Sodium Pump	6 [33]	0.60
	Chloride Salts Pump	4	1.00
	Particle lifting system	8 [17]	0.50 [17]
	sCO_2 Power Block	4 [34], [35]	0.75

The SRL is calculated as the average of the component SRL values. The maturity score is calculated using Equation (5) identifying the SRL_{max} and SRL_{min} in the set of layouts analysed.

$$S_{mat} = \frac{4 \cdot (SRL - SRL_{min})}{SRL_{max} - SRL_{min}} + 1 \quad (5)$$

The safety score (S_{safe}) benchmarks a specific CSP+sCO_2 layout based on the safety issues. Five main safety concerns have been considered based on the media employed in the receiver and the storage: toxicity (f_{tox}), flammability (f_{flam}), high-pressures (f_{hp}), corrosion (f_{corr}), and structural concerns (f_{struc}). Each of these factors is calculated as the average between the two factors defined for the receiver and the storage, reported in Table 2. The higher the factor, the more critical is the problem related to the medium employed. The safety score is calculated as shown in Equation (6) and the higher the value, the safer is the configuration analyzed.

$$S_{safe} = 5 - \sum_{i=1}^{5} f_i \quad (6)$$

The complexity of a configuration is defined based on the number of components per layout (number of components factor (f_{nc})) and the manufacturing issues and/or lack of experience for each component (component complexity factor (f_{cc})). On one side, the first factor is defined assuming that the higher the number of components (nc), the higher the complexity of the system, as well as the risk of failures (Equation (7)). On the other side, the components complexity factor is calculated as the average between all the component factors of the components employed in a specific system layout (Equation (8)). The assumed values for these factors are reported in Table 3 and Table 4. Therefore, the complexity score is calculated as shown in Equation (9).

$$f_{nc} = \frac{4 \cdot (nc - nc_{min})}{nc_{max} - nc_{min}} + 1 \quad (7) \qquad f_{cc} = \frac{\sum_{i=1}^{n} component\ factor_i}{n} \quad (8) \qquad S_{comp} = 5 - \frac{f_{nc} + f_{cc}}{2} \quad (9)$$

The maximum temperature score (S_{temp}) quantifies the potential energy-conversion efficiency that can be achieved by employing a specific receiver and/or storage type. The highest score corresponds to the highest temperature theoretically achievable in the two subsystems. For a given plant layout, the Receiver Temperature Score and the Storage Temperature Score have been defined based on the subsystem theoretical temperatures identified in the literature and reported in Table 2. The temperature scores are then calculated as shown in Equation (10) and (11) based on the lowest and the highest temperature values (T_{min} and T_{max}). The maximum temperature score is calculated as the average between the scores.

$$S_{temp,REC} = \frac{4 \cdot \left(T_{REC} - T_{REC,min}\right)}{T_{REC,max} - T_{REC,min}} + 1 \quad (10) \qquad S_{temp,TES} = \frac{4 \cdot \left(T_{TES} - T_{TES,min}\right)}{T_{TES,max} - T_{TES,min}} + 1 \quad (11)$$

RESULTS AND DISCUSSIONS

A comparison between the proposed CSP+sCO2 layouts and the selection of the most attractive ones is presented in this section. Figure 3 shows the maturity, potential-low cost, maximum temperature, safety, and system complexity scores for the configurations investigated classified by the receiver HTF. As expected, the point of strength of molten salt-based layouts is their maturity, while due to the limits on the medium chemical stability, they are characterized by the lowest maximum temperature score. Air-based systems coupled with packed-bed TES stand out for their potential low cost and the highest maximum temperature achievable, while their points of weakness are system complexity and low maturity. The layouts employing particles share the same weaknesses with the air-based layouts but they have been benchmarked as the safest and as low-cost systems. Sodium-based configurations have been classified as mature as particle-based systems, but more complex, with more safety issues, more expensive, and with lower operating temperatures. The configurations employing chloride salt and CO_2 as HTF in the receiver have been classified as the least mature in this analysis. Additionally, the chloride salt-based layouts are the most expensive configurations. The CO_2 systems stand out for their relatively high temperature and potentially low cost.

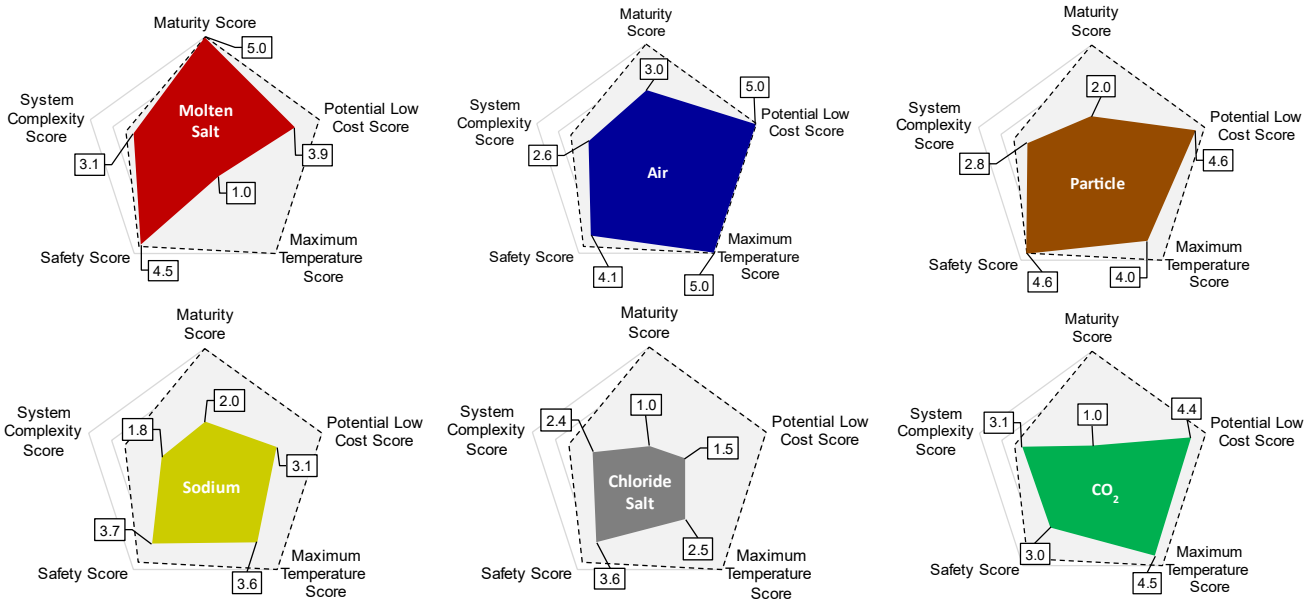

Figure 3: Intermediate scores of the layouts investigated classified by the receiver HTF

The intermediate scores have been combined in an overall score by using the three combinations of weights identified in the methodology: *Best for Maturity*, *Best for Cost*, and *Maturity/Cost*. Figure 4 shows the overall score values for the best layouts for each receiver heat transfer fluid as a function of the three considered weight combinations. The molten salt layout would be the most attractive one if maturity was prioritized, while the air-based systems would stand out if the cost was prioritized. Layouts employing particles reach the third-highest score regardless of the weights combinations. Comparing the sodium and CO_2 score values, sodium has a higher overall score if maturity is prioritized, otherwise, the opposite can be stated. The chloride salt is the least attractive configuration for the three combinations of weights.

The Maturity/Cost combination offers an average trend that takes into account the spread of the overall scores as a function of the two extreme weight combinations and it has been chosen to benchmark the proposed layouts. The overall scores of the layouts proposed in this analysis are presented in Figure 5, highlighting the share of each intermediate score.

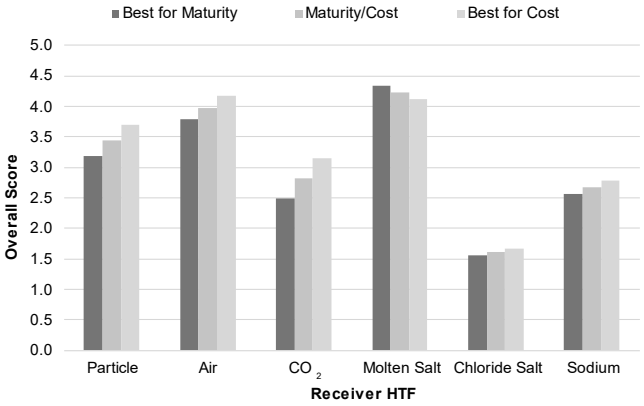

Figure 4: Sensitivity Analysis of the score weights

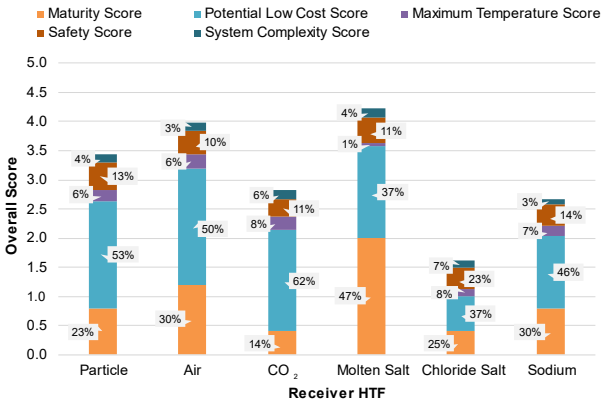

Figure 5: Overall score breakdown - Maturity/Cost

Therefore, through the defined analytical approach, based on techno-economic criteria and the definition of an overall score for each layout investigated, the best three CSP+sCO2 plant configurations have been selected. The molten salt layout has been identified as the most attractive configuration with the highest overall score equal to 4.2. This configuration is the closest to the state-of-the-art and it represents the first step towards a new generation of CSP plants. Air and particle layouts are the second and the third layout with the highest overall score, respectively equal to 4.0 and 3.8. They have similar shares for the potential low-cost score, while the air has a larger share for the maturity score (30% vs 23%). Air- and particle-based systems are the other two most attractive CSP+sCO2 configurations that can drive towards a lower cost of electricity thanks to their lower costs and better energy performances. The low weight assigned to the temperature score implies that maturity and costs have been deliberately favored over efficiency. Consequently, the potential of the air- and particle-based systems, which have the highest operating temperatures, could have been underestimated. In addition, the circularity and the environmental impact of the systems in this analysis have been only partially included and limited to toxicity and flammability. Strengthening this criterion, particle systems would be favored, followed by air ones, which can leverage by the use of harmless and free HTF, and waste media in the TES.

CONCLUSIONS

In this work, a methodology to identify the most promising CSP layouts to be Integrated with sCO_2 power cycles has been introduced. Twenty-one sCO2 – CSP connection layouts have been identified, classified by the receiver heat transfer fluid and storage design, and benchmarked with an overall score based on techno-economic criteria. Results show that the layout with a molten salt receiver and a double tank molten salt storage is the most attractive. This configuration stands out for its maturity and covers a gap between the state-of-the-art and the new generations of CSP plants. The main limitation of this layout is the relatively low maximum temperature that can be achieved by conventional molten salts. The other two most attractive configurations are the air- and particle-based systems including air packed bed or particles silos TES. The potential low cost and the maximum operating temperatures are the main drivers for these systems, that can enhance the economic competitiveness of CSP plants.Techno-economic models will be implemented for the most promising layouts identified in this study, including hybridization with PV field and with the grid to make the most of the TES included in the CSP plant.

ACKNOWLEDGEMENTS

The authors acknowledge the financial support from the European Union's Horizon 2020 research and innovation program, project No.952953.

REFERENCES

[1] S. Trevisan, R. Guédez, and B. Laumert, “Thermo-economic optimization of an air driven supercritical CO2 Brayton power cycle for concentrating solar power plant with packed bed thermal energy storage,” *Sol. Energy*, vol. 211, no. October, pp. 1373–1391, 2020, doi: 10.1016/j.solener.2020.10.069.

[2] M. F. Austin and D. M. York, “System Readiness Assessment (SRA) an illustrative example,” *Procedia Comput. Sci.*, vol. 44, no. C, pp. 486–496, 2015, doi: 10.1016/j.procs.2015.03.031.

[3] M. Héder, “From NASA to EU: The evolution of the TRL scale in Public Sector Innovation,” *Innov. J.*, vol. 22, no. 2, pp. 1–23, 2017.

[4] A. Bonk, M. Braun, V. A. Sötz, and T. Bauer, “Solar Salt – Pushing an old material for energy storage to a new limit,” *Appl. Energy*, vol. 262, no. January, p. 114535, 2020, doi: 10.1016/j.apenergy.2020.114535.

[5] M. Mehos *et al.*, “Concentrating Solar Power Gen3 Demonstration Roadmap,” *NREL/Tp-5500-67464*, no. January, pp. 1–140, 2017, doi: 10.2172/1338899.

[6] C. W. Forsberg, P. F. Peterson, and H. Zhao, “High-temperature liquid-fluoride-salt closed-Brayton-cycle solar power towers,” *J. Sol. Energy Eng. Trans. ASME*, vol. 129, no. 2, pp. 141–146, 2007, doi: 10.1115/1.2710245.

[7] R. W. Bradshaw *et al.*, “Final Test and Evaluation Results from the Solar Two Project,” *Contract*, no. January, p. 294, 2002, doi: 10.2172/793226.

[8] J. M. Christian and C. K. Ho, “CFD simulation and heat loss analysis of the solar two power tower receiver,” *ASME 2012 6th Int. Conf. Energy Sustain. ES 2012, Collocated with ASME 2012 10th Int. Conf. Fuel Cell Sci. Eng. Technol.*, no. PARTS A AND B, pp. 227–235, 2012, doi: 10.1115/ES2012-91030.

[9] G. Zhu and C. Libby, “Review and future perspective of central receiver design and performance,” *AIP Conf. Proc.*, vol. 1850, no. June 2017, doi: 10.1063/1.4984395.

[10] P. Požívil, V. Aga, A. Zagorskiy, and A. Steinfeld, “A pressurized air receiver for solar-driven gas turbines,” *Energy Procedia*, vol. 49, pp. 498–503, 2014, doi: 10.1016/j.egypro.2014.03.053.

[11] H. N. Kim *et al.*, “Experimental evaluation of the performance of solar receivers for compressed air,” *J. Mech. Sci. Technol.*, vol. 28, no. 11, pp. 4789–4795, 2014, doi: 10.1007/s12206-014-1046-x.

[12] R. Osuna *et al.*, “SOLAIR: Advanced Solar Volumetric Air Receiver for Commerical Solar Tower Power Plants,” *Tech. Rep.*, no. January 2005, pp. 1–12, 2005.

[13] K. Armijo, “Design Basis for a 2.0MWth Liquid-HTF Pilot- Scale CSP System,” 2019.

[14] G. Mohan, M. Venkataraman, J. Gomez-Vidal, and J. Coventry, “Assessment of a novel ternary eutectic chloride salt for next-generation high-temperature sensible heat storage,” *Energy Convers. Manag.*, vol. 167, pp. 156–164, 2018, doi: 10.1016/j.enconman.2018.04.100.

[15] J. Coventry, C. Andraka, J. Pye, M. Blanco, and J. Fisher, “A review of sodium receiver technologies for central receiver solar power plants,” *Sol. Energy*, vol. 122, pp. 749–762, 2015, doi: 10.1016/j.solener.2015.09.023.

[16] S. Guccione, R. Guedez, J. Pye, L. Savoldi, and R. Zanino, “Design and Optimization of a Sodium-Molten Salt Heat Exchanger for Concentrating Solar Power applications,” 2020.

[17] J. M. Christian, J. Sment, C. K. Ho, L. Haden, and K. Albrecht, “Particle lift challenges and solutions for solid particle receiver systems,” *ASME 2019 13th Int. Conf. Energy Sustain. ES 2019, collocated with ASME 2019 Heat Transf. Summer Conf.*, pp. 1–8, 2019, doi: 10.1115/ES2019-3833.

[18] C. Ho *et al.*, “Technology advancements for next-generation falling particle receivers,”

Energy Procedia, vol. 49, pp. 398–407, 2014, doi: 10.1016/j.egypro.2014.03.043.
[19] C. K. Ho, “A review of high-temperature particle receivers for concentrating solar power,” *Appl. Therm. Eng.*, vol. 109, pp. 958–969, 2016, doi: 10.1016/j.applthermaleng.2016.04.103.
[20] J. D. Osorio, R. Hovsapian, and J. C. Ordonez, “Dynamic analysis of concentrated solar supercritical CO2-based power generation closed-loop cycle,” *Appl. Therm. Eng.*, vol. 93, pp. 920–934, 2016, doi: 10.1016/j.applthermaleng.2015.10.039.
[21] J. D. Ortega and J. M. Christian, “Design Requirements for Direct Supercritical Carbon Dioxide,” *Proc. 9th Int. Conf. Energy Sustain.*, pp. 1–6, 2015.
[22] J. Ortega, S. Khivsara, J. Christian, C. Ho, J. Yellowhair, and P. Dutta, “Coupled modeling of a directly heated tubular solar receiver for supercritical carbon dioxide Brayton cycle: Optical and thermal-fluid evaluation,” *Appl. Therm. Eng.*, vol. 109, pp. 970–978, 2016, doi: 10.1016/j.applthermaleng.2016.05.178.
[23] J. Ortega, S. Khivsara, J. Christian, C. Ho, and P. Dutta, “Coupled modeling of a directly heated tubular solar receiver for supercritical carbon dioxide Brayton cycle: Structural and creep-fatigue evaluation,” *Appl. Therm. Eng.*, vol. 109, pp. 979–987, 2016, doi: 10.1016/j.applthermaleng.2016.06.031.
[24] S. C. Johnson *et al.*, “Selecting favorable energy storage technologies for Nuclear power,” in *Storage and Hybridization of Nuclear Energy: Techno-economic Integration of Renewable and Nuclear Energy*, Elsevier Inc., 2018, pp. 119–175.
[25] B. Cárdenas *et al.*, “Techno-economic optimization of a packed-bed for utility-scale energy storage,” in *Applied Thermal Engineering*, vol. 153, 2019, pp. 206–220.
[26] S. Flueckiger, Z. Yang, and S. V. Garimella, “An integrated thermal and mechanical investigation of molten-salt thermocline energy storage,” *Appl. Energy*, vol. 88, no. 6, pp. 2098–2105, 2011, doi: 10.1016/j.apenergy.2010.12.031.
[27] International Renewable Energy Agency, “Thermal Energy Storage Technology Brief E17,” no. January 2013.
[28] CORDIS EU Research, L. Und, and R. Ev, “COMPONENTS ’ AND MATERIALS ’ PERFORMANCE FOR ADVANCED SOLAR SUPERCRITICAL CO2 POWERPLANTS.” pp. 1–5, 2020, [Online]. Available: https://cordis.europa.eu/project/id/958418.
[29] CORDIS EU Research, “Novel high-performance materials and components (RIA).” pp. 6–7, 2019, [Online]. Available: https://cordis.europa.eu/programme/id/H2020_LC-SPIRE-08-2020.
[30] J. S. Al-Ansary H and A.-S. Z. Sadowski D, Alrished A, Golob M, El-Leathy A, “Experimental Study of a Sand-Air Heat Exchanger for user with a High-Temperature Solar Gas Turbine System,” 2011.
[31] Golob et Al., “Serpentine Particle-Flow Heat Exchanger with Working Fluid, for Solar Thermal Power Generation,” 2013.
[32] E. U.-H. 2020, “SOLAR based sCO2 Operating Low-cost plants,” 2020. https://cordis.europa.eu/project/id/952953.
[33] J. Coventry, C. Andraka, J. Pye, M. Blanco, and J. Fisher, “A review of sodium receiver technologies for central receiver solar power plants,” *Sol. Energy*, vol. 122, pp. 749–762, 2015, doi: 10.1016/j.solener.2015.09.023.
[34] R. V. Padilla, Y. C. Soo Too, R. Benito, and W. Stein, “Exergetic analysis of supercritical CO2 Brayton cycles integrated with solar central receivers,” *Appl. Energy*, vol. 148, pp. 348–365, 2015, doi: 10.1016/j.apenergy.2015.03.090.
[35] R. Vasquez Padilla *et al.*, “Performance Analysis of a Rankine Cycle Integrated With the Goswami Combined Power and Cooling Cycle,” *J. Energy Resour. Technol.*, vol. 134, no. 3, pp. 1–8, 2012, doi: 10.1115/1.4006434.